Biophysical Journal Volume 68 February 1995 634–647

Grand Canonical Monte Carlo Molecular and Thermodynamic Predictions of Ion Effects on Binding of an Oligocation (L^{8+}) to the Center of DNA Oligomers

Martha C. Olmsted,* Jeffrey P. Bond,* Charles F. Anderson,* and M. Thomas Record, Jr.*‡
Departments of *Chemistry and ‡Biochemistry, University of Wisconsin–Madison, Madison, Wisconsin 53706 USA

ABSTRACT Grand canonical Monte Carlo (GCMC) simulations are reported for aqueous solutions containing excess univalent salt (activities $a_{\pm}$ = 1.76–12.3 mM) and one of the following species: an octacationic rod-like ligand, L^{8+}; a B-DNA oligomer with N phosphate charges ($8 \leq N \leq 100$); or a complex resulting from the binding of L^{8+} at the center of an N-mer ($24 \leq N \leq 250$). Simplified models of these multiply charged species are used in the GCMC simulations to predict the fundamental coulombic contributions to the following experimentally relevant properties: 1) the axial distance over which ligand binding affects local counterion concentrations at the surface of the N-mer; 2) the dependence on N of GCMC preferential interaction coefficients, $\Gamma_{32}^{MC} \equiv \partial C_3/\partial C_2|_{a_{\pm},T}$, where C_3 and C_2 are, respectively, the molar concentrations of salt and the multiply charged species (ligand, N-mer or complex); and 3) the dependence on N of $S_aK_{obs} \equiv$ d ln K_{obs}/d ln $a_{\pm} = \Delta(|Z_J| + 2\Gamma_{32J})$, where K_{obs} is the equilibrium concentration quotient for the binding of L^{8+} to the center of an N-mer and Δ denotes the stoichiometric combination of terms, each of which pertains to a reactant or product J having $|Z_J|$ charges. The participation of electrolyte ions in the ligand binding interaction is quantified by the magnitude of S_aK_{obs}, which reflects the net (stoichiometrically weighted) difference in the extent of thermodynamic binding of salt ions to the products and reactants. Results obtained here from GCMC simulations yield a picture of the salient molecular consequences of binding a cationic ligand, as well as thermodynamic predictions whose applicability can be tested experimentally. Formation of the central complex is predicted to cause a dramatic reduction in the surface counterion (e.g., Na^+) concentration over a region including but extending well beyond the location of the ligand binding site. For binding a cationic ligand, S_aK_{obs} is predicted to be negative, indicating net electrolyte ion release in the binding process. At small enough N, $-S_aK_{obs}$ is predicted to decrease strongly toward zero with decreasing N. At intermediate N, $-S_aK_{obs}$ appears to exceed its limiting value as $N \rightarrow \infty$.

INTRODUCTION

Interactions of oligocationic ligands, including both inorganic cations (e.g., Mg^{2+}, $Co(NH_3)_6^{3+}$) and organic cations (e.g., polyamines, oligopeptides) with polymeric nucleic acids in solution have been investigated by thermodynamic and spectroscopic methods, because these systems are of intrinsic biological or biochemical significance and/or because they may be useful models for the coulombic component of protein-nucleic acid interactions. The association of an oligocation with a nucleic acid may be described by the quotient K_{obs}, expressed in terms of the equilibrium concentrations of the participants in the reaction L + D $\rightleftarrows$ LD, where L is the oligocationic ligand, D represents DNA, and LD the complex. Spectroscopic and thermodynamic studies of binding of oligocations to polymeric DNA demonstrate strong dependence on univalent salt activity both of the local ligand concentration (as monitored by spectroscopic probes, e.g., Padmanabhan et al., 1990, 1991) and of K_{obs} (cf. Record et al., 1976, 1978, 1990; Lohman and Mascotti, 1992). At both the molecular and thermodynamic levels, these oligocation-polyanion interactions behave experimentally as ion exchange processes in which association of the oligocation causes a reduction in the local gradients of salt ions, notably in the preexisting cation concentration gradient in the vicinity of DNA (the polyelectrolyte effect; cf. Record et al., 1991; Bond et al., manuscript in preparation).

Under the conditions of interest here, the effect of the activity ($a_{\pm}$) of excess salt on K_{obs} for any equilibrium involving charged species can be expressed by the relationship (Anderson and Record, 1993; Record and Anderson, 1995)

$$\left(\frac{\partial \ln K_{obs}}{\partial \ln a_{\pm}}\right)_{T,P} \equiv S_aK_{obs} = \Delta(|Z_J| + 2\Gamma_{32J}). \quad (1)$$

In the present application of Eq. 1, Γ_{32J} is the preferential interaction coefficient describing the thermodynamic consequences of interactions between the electrolyte component (3) and the electroneutral component 2J, where J denotes one of the participants, with charge Z_J, in the binding reaction (oligocation, oligomeric nucleic acid, or their complex). The following section (Theoretical Background) provides more explicit definitions and commentary on the physical significance of Γ_{32} and S_aK_{obs}.

If the polyelectrolyte effect is the dominant origin of the dependence of K_{obs} on salt activity for binding of an oligocation to the DNA polymer, as first proposed by Record et al.

Received for publication 9 September 1994 and in final form 21 November 1994.

Address reprint requests to M. Thomas Record, Jr., Department of Biochemistry, University of Wisconsin, 420 Henry Mall, Madison, WI 53706. Tel.: 608-262-5332; Fax: 608-262-3453; E-mail: record@chem.wisc.edu.

Dr. Olmsted's current address: University of Colorado, Health Sciences Center, Department of Biochemistry, Biophysics and Genetics, 4200 E. 9th Avenue, Denver, CO 80262.

0006-3495/95/02/634/14 $2.00

(1976), then the magnitude of S_aK_{obs} should be greatly reduced for binding of that ligand to sufficiently short oligomers of DNA, which do not exhibit the extreme local ion concentration gradients and high surface cation concentration characteristic of polymeric DNA (Olmsted et al., 1989). A quantitative investigation of the N-dependence of S_aK_{obs} is a primary component of the present computational study. GCMC simulations are used to predict both molecular and thermodynamic aspects of the complexation of an oligocation (here L^{8+}) at the center of B-DNA oligoanions of various lengths ($8 \leq N \leq 250$). We have examined the simplest structural model that can represent the effects of complex formation on properties that are determined (at least to a large extent) by long range coulombic interactions. The ligand and DNA oligomer are modeled as cylinders of uniform axial charge density, and the complex is modeled by elimination of the eight central charges on the oligomer. On the basis of these and other standard model assumptions, we calculate axial profiles of surface counterion concentrations at $a_\pm$ = 1.76 mM, and preferential interaction coefficients (Γ_{32J}) at two activities of univalent salt ($a_\pm$ = 1.76 mM and 12.3 mM) for each of the three participants in the binding equilibrium: L^{8+}, DNA oligomer, the central complex of L^{8+} with the DNA oligomer. GCMC calculations of Γ_{32J} are also reported for DNA oligomers at an intermediate $a_\pm$ (7.07 mM). The predicted axial profiles of the counterion concentration at the N-mer surface provide one view of the molecular consequences of ion exchange from N-mers of various lengths. With the predicted values of Γ_{32J}, the experimentally measurable thermodynamic quantity S_aK_{obs} is evaluated as a function of N.

THEORETICAL BACKGROUND: PREFERENTIAL INTERACTION COEFFICIENTS

Of the various thermodynamic coefficients that are quantitative measures of nonideality in solutions containing univalent salt ions and oligo- (or poly-)electrolytes, the preferential interaction coefficient Γ_{32} is uniquely useful as an experimentally and theoretically determinable measure of the thermodynamic consequences of interactions between the electrolyte component (designated "3") and an electroneutral component "2." (In the present application component "2" is comprised of any of the three types of oligoions (L, D, LD), together with a neutralizing complement of univalent counterions, not site-bound to the oligoion.) Applications of preferential interaction coefficients to predict and to analyze effects of salt concentration on the transition temperatures of various order-disorder transitions of oligomeric and polymeric nucleic acid helices have been made by Olmsted et al. (1991) and Bond et al. (1994).

The role of preferential interaction coefficients in the thermodynamic analysis of salt effects on equilibria involving charged polymers has been rigorously established for systems in which all solute components are dilute in comparison to the concentration of excess salt (Anderson and Record, 1993). In particular, the condition of high dilution in all reactants and products ensures that each in turn can be viewed as the nondiffusible component in a three-component solution containing excess salt and solvent, for the purpose of describing its interactions with salt by means of a preferential interaction coefficient. For a three-component system, Γ_{32} can be identified with the Donnan coefficient that can (at least in principle) be evaluated by equilibrium membrane dialysis experiments, which quantify differences in the salt concentration C_3 across a membrane impermeable to component 2 as a function of its concentration, C_2 (see for example Record and Anderson, 1995). When component "2" is sufficiently dilute, C_3 becomes a linear function of C_2 under the "Donnan" constraints of constant temperature (T) and constant chemical potentials of the salt and solvent (μ_3 and μ_1, respectively). Under these experimentally accessible conditions, the Donnan coefficient can be evaluated as the derivative

$$\Gamma^{o}_{32} = \lim_{C_2 \to 0} \left(\frac{\partial C_3}{\partial C_2} \right)_{\mu_1, \mu_3, T}. \tag{2}$$

In both experimental measurements and theoretical calculations, Donnan coefficients and preferential interaction coefficients are most conveniently expressed on the molar concentration scale. In the context of certain thermodynamic derivations, use of the molal concentration scale to define Γ both simplifies the development and yields simpler final expressions (Anderson and Record, 1993; Record and Anderson, 1995).

To simplify notation designating preferential interaction coefficients in this paper the superscript "o," which denotes the limit of low C_2, and the subscript "32" will be understood, because the only type of preferential interactions considered are those of a univalent salt component with a sufficiently dilute electroneutral component involving either L^{8+}, a DNA N-mer, or their complex. The corresponding preferential interaction coefficients are compactly and unambiguously designated $\Gamma_{|Z_J|}$, where Z_J is the number of structural univalent charges on species J, and $|Z_{LD}| = |Z_D| - |Z_L|$. (For the purposes of the present development, the possibility that salt ions could site-bind either to D or to L is not considered.) For oligo- or polyelectrolytes of known Z, experimental values and theoretical predictions of preferential interaction coefficients can be expressed either on a molecule or charge basis, as dictated by convenience. These expressions are related by

$$\Gamma_{|Z|,u} = \Gamma_{|Z|}/|Z| \tag{3}$$

where

$$\Gamma_{|Z|,u} \equiv \lim_{C_u \to 0} \left(\frac{\partial C_3}{\partial C_u} \right)_{\mu_1, \mu_3, T} \tag{4}$$

and $C_u \equiv |Z| C_2$. The symbol Γ will be used when general comments about preferential interaction coefficients are

made. For systems in which coulombic interactions are dominant, Γ is invariably negative, reflecting net exclusion of the salt component in a Donnan equilibrium.

The simplest theoretical method of predicting Γ is based on the concept of counterion condensation (CC), which yields limiting forms of Γ^{CC} at sufficiently low concentrations of (excess) salt in solutions of sufficiently dilute cylindrical polyions that are long enough to be considered effectively infinite (Manning, 1969). For a given solvent, temperature, and counterion charge type, the limiting forms of Γ^{CC} depend only on the average axial charge density of the cylindrical polyion. These analytic expressions for Γ^{CC} are identical to those obtained from the Poisson-Boltzmann (PB) cylindrical cell model without use of the condensation hypothesis (Anderson and Record, 1980, 1983). From Fixman's (1979) investigation of the range of validity of the PB approximation, it follows that the limiting law expressions for Γ^{CC} are rigorous (given the model assumptions), but their accuracy at typical experimental concentrations is not guaranteed. Of the more general theoretical methods that could be used to predict Γ, the two currently prevalent are based either on the PB equation or on grand canonical Monte Carlo (GCMC) simulations (Mills et al., 1986).

There are (at least) four distinct ways in which Γ can be evaluated from calculations based on the PB equation. 1) For an isolated cylindrical polyion the second virial coefficient can be evaluated by integrating numerical solutions of the cylindrical PB equation (Stigter, 1975). 2) The linkage equation derived from the PB cell model for a cylindrical polyion by Anderson and Record (1980) can be differentiated directly, under the constraints of constant electrolyte activity and temperature, to obtain $\Gamma^{PB} \equiv (\partial C_3/\partial C_u)_{a_\pm,T}$ (Anderson and Record, 1983). 3) Subject to these constraints, numerical integrations of solutions of the cylindrical PB equation can be used to calculate C_3 as a linear function of C_u, so that Γ^{PB} can be evaluated directly as the slope of a plot of C_3 vs. C_u (Mills et al., 1986). 4) By appropriate numerical integrations the excess electrostatic free energy attributable to the interactions of salt ions with a multiply charged species (of arbitrary structure) can be evaluated and then numerically differentiated with respect to salt concentration to obtain a derivative that is approximately equivalent to Γ (Misra et al., 1994). All methods based on the PB equation entail the neglect of certain interionic correlations. At sufficiently high dilutions this PB approximation becomes exact (Fixman, 1979), but its accuracy in the usual experimental range of concentrations can be assessed best from a comparison with actual measurements (or with GCMC simulations, as discussed below). The reliability of the PB approximation varies considerably with the property to be calculated (Anderson and Record, 1990).

For a given set of model assumptions Monte Carlo (MC) methods generally provide the only definitive means of testing for a particular application the theoretical accuracy of the PB approximation (or of other analytic alternatives, such as the hypernetted chain equation (Bacquet and Rossky, 1984; Murthy et al., 1985)). Mills et al. (1986) and Olmsted et al. (1989, 1991) have developed GCMC methods to calculate Γ_{32J} for cylindrical models of polymeric and oligomeric electrolytes. By analogy to the third way of calculating Γ^{PB} described above, $\Gamma^{MC} \equiv (\partial C_3/\partial C_u)_{a_\pm,T}$ can be evaluated as the slope of a plot of C_3 vs. C_u, as determined by an appropriate series of GCMC simulations (Mills et al., 1986). For any model that neglects the molecularity of the solvent, neither μ_1 nor pressure can be explicitly controlled while C_u is varied. Thus, the approximations entailed in the identification of Γ^{MC} (or Γ^{PB}) with Γ are not obvious. This issue has been addressed by Anderson and Record (1993), who examined the thermodynamic foundation for the use of GCMC simulations in the calculation of Γ for the standard (primitive) model of a polyelectrolyte-salt solution. These considerations pertain equally well to the model solutions containing oligoelectrolytes that are of interest in the present study.

The GCMC simulations reported by Olmsted et al. (1989) for a homologous series of oligoelectrolytes (model DNA oligomers, designated N-mers having $|Z_D| = N$ charges) predicted that the positive quantity $-\Gamma_{N,u}$ decreases with increasing N. For large enough N, $\Gamma_{N,u}$ approaches the corresponding polyelectrolyte value ($\Gamma_{\infty,u}$) as a linear function of N^{-1}

$$-\Gamma_{N,u} = -\Gamma_{\infty,u} + \alpha/N. \tag{5}$$

Here the constant (N-independent) parameter α depends on $a_\pm$ and on the structural characteristics common to each (model) N-mer in the series (b, the average axial intercharge distance and a, the radial distance of closest approach of ion centers to the N-mer axis; Olmsted et al., 1991). (Previously we have used the symbol "D" instead of α in Eq. 5; in the present paper D refers exclusively to a DNA oligomer.) The magnitude of α is a measure of the oligo- "end effect" on Γ, which causes the preferential interaction coefficient (expressed per monomer) of an N-mer to deviate from the value characteristic of the corresponding polymer.

For the binding of L to a DNA oligomer (D) to form the complex LD, Eq. 1 has the explicit form

$$\begin{aligned} S_a K_{obs} = [&(|Z_{LD}| + 2\Gamma_{|Z_{LD}|}) \\ &- (|Z_L| + 2\Gamma_{|Z_L|}) - (|Z_D| + 2\Gamma_{|Z_D|})]. \end{aligned} \tag{6}$$

Since $|Z_{LD}| = |Z_D| - |Z_L|$, this equation can be expressed more compactly as

$$S_a K_{obs} = 2(\Gamma_{|Z_{LD}|} - \Gamma_{|Z_L|} - \Gamma_{|Z_D|}) - 2|Z_L|. \tag{7}$$

However, the physical interpretation of the groups of terms in Eq. 6 is more straightforward. Each term ($|Z| + 2\Gamma_{|Z|}$) may be interpreted as the "thermodynamic extent of association" of univalent counterions (cations or anions, as appropriate) with the indicated oligoelectrolyte species (nucleic acid, ligand or complex) (Anderson and Record, 1982, 1993; Record and Anderson, 1995). ("Thermodynamic extent of association" does not imply site binding of counterions, but

rather is descriptive of the thermodynamic nonideality of the ion gradients in the vicinity of the poly- (or oligo-) ion, which make it thermodynamically equivalent to a weak electrolyte with $|Z| + 2\Gamma_{|Z|}$ undissociated counterions.) Therefore, on the basis of Eq. 6, S_aK_{obs} may be viewed as the result of two thermodynamic contributions: one from the release of anions from the ligand L upon complexation, given by $|Z_L| + 2\Gamma_{|Z_L|}$; the other from the release of cations from the DNA upon complexation, given by $(|Z_D| + 2\Gamma_{|Z_D|}) - (|Z_{LD}| + 2\Gamma_{|Z_{LD}|})$.

METHODS

Model

We adopt here the standard primitive model for a three-component solution consisting of water, univalent cations, and anions, and a multiply charged cylindrical molecule representing either an oligoanionic nucleic acid, the oligocationic ligand L^{8+}, or their complex. The assumptions comprising this model and its utility for various applications have been considered in some detail elsewhere (Anderson and Record, 1990). For this model the magnitude of Γ is determined entirely by long range coulombic interactions (subject to excluded volume boundary conditions). At sufficiently large values of $a_{\pm}$, changes in noncoulombic interactions of salt ions (e.g., Hofmeister effects) as well as changes in hydration upon complexation can contribute to the magnitude of experimental values of S_aK_{obs} (cf. Record and Anderson, 1995). Changes in hydration may also contribute additional terms to Eq. 1 (Anderson and Record, 1993), but these are not expected to be significant in the range of salt concentrations considered here.

In accord with the usual standard model assumptions, the univalent cations and anions are modeled as uniformly charged impenetrable spheres, both with a radius of 3 Å (taken to represent hydrated ionic radii; Mills et al. 1985). The entire solution is modeled as a dielectric continuum with dielectric constant $\epsilon = 78.7$, the value characteristic of pure water at 25°C. Since only coulombic (charge-charge) and hard particle interactions are considered in evaluation of the configuration energy, the temperature enters into the GCMC simulation only as the product ϵT. At 40°C ϵT is only 4% smaller than its value at 5°C. Thus, at any of the temperatures where DNA-ligand binding isotherms are typically measured, the difference between ϵT and its value at 25°C is expected to be insignificant for the present application.

The charge distribution on a B-DNA oligomer with N monomeric units (N-mer; $8 \leq N \leq 100$) is modeled as $|Z|$ discrete axial unit charges ($|Z| = N$) separated by a uniform spacing of 1.7 Å, the distance between adjacent phosphate charges projected onto the helical axis of B-DNA. For the GCMC simulations described below, the N-mer is assumed to exclude a cylindrical volume to the ion centers, so that the distance of closest approach to the cylinder axis in the radial direction (a) is 13 Å and the axial distance of closest approach to the terminal charge on the N-mer is 6 Å. (The volume excluded by a cylindrical object to a sphere is not itself precisely cylindrical, but the difference is negligible for the range of dimensions considered here.) The structural parameters assigned to the DNA N-mer are plausible choices that were assumed here for consistency with previous MC simulations (Olmsted et al., 1989, 1991). In the absence of any explicit experimental information about the structure of the free oligocation L^{8+} in solution, for simplicity it is modeled here as having the same structure and charge density as a B-DNA 8-mer, but with positive charges. The charge assigned to the ligand ($Z_L = 8$) was chosen to facilitate accurate computations (smaller values of Z_L resulted in a larger relative error in S_aK_{obs}) and because it is within the range of Z_L that has been investigated experimentally. A preliminary study using the spherical PB equation to assess the effect of ligand size (at constant Z_L) on the magnitude of S_aK_{obs} suggests that it is of secondary importance ($\lesssim$10% for $N = 72$). This issue will be addressed more systematically in a following paper (Bond et al., manuscript in preparation).

To implement the application of Eq. 1 for the purpose of calculating S_aK_{obs}, the ligand is taken to be in either of two states: bound to the center of a DNA N-mer, or completely free in bulk solution. The L^{8+}-N-mer complex (LD) is modeled by removing 8 consecutive unit charges centered on the midpoint of the N-mer ($|Z_{LD}| = N - 8$, $24 \leq N \leq 250$). The radial distance of closest approach of the small ions to the cylindrical axis of LD is taken to be uniform over its entire length, including the site of complexation. Neglecting any difference between the volume excluded to ion centers by LD and D in effect introduces an artificially large decrease in the volume excluded to the salt ions as a result of complex formation. This effect may be corrected for approximately by adding $2C_3^{\circ}\Delta V_u$ to S_aK_{obs}, where ΔV_u is the difference in volume excluded to ion centers by the oligoionic species (Anderson and Record, 1993). At the salt activities studied here this correction results in changes in S_aK_{obs} (<3%) that are within the statistical error of GCMC determinations of this quantity.

GCMC methods

The objective of each GCMC simulation is to generate a Markov chain of configurations of the model solution at specified $a_{\pm}$, T, and volume in such a way that certain equilibrium properties (here the average concentration of coions in the cell, C_3, and the surface concentration of counterions, $C_{|Z|}(a)$, as a function of axial position) can be determined from averages over the configurations. A trial configuration of the system, with a different configurational energy, is generated from the current configuration by attempting randomly one of the following transitions: moving one or more salt ions, or inserting or deleting an electroneutral collection of salt ions. The next configuration (either the trial or the current configuration) is chosen using an acceptance probability appropriate for the grand canonical ensemble. For a given type of transition the acceptance probability depends only on $a_{\pm}$, ϵT, the energy difference between the two configurations, the volume available to the ion centers, and the number of each type of ion in the configuration. More specific details of our GCMC simulations for model salt solutions containing a cylindrical polyion have been summarized by Mills et al. (1986). Valleau and Whittington (1977) review the use of Metropolis Monte Carlo methods in statistical mechanics; Valleau and Cohen (1980) describe the GCMC method with specific applications to primitive model simulations of salt solutions in the absence of oligo- (or poly-) electrolytes.

For the simulations reported here, the MC cell is a rectangular prism (in some cases a cube) containing, in addition to a fluctuating number of small mobile ions, a single fixed N-mer or LD complex, the center of which coincides with the center of the simulation cell and the axis of which coincides with the long axis of the simulation cell. The side lengths of the cell are $2R_{xy}$ (perpendicular to the oligoion axis) and $2R_z$ (parallel to the oligoion axis) so that the concentration of oligoion charges $C_u = |Z_J| 10^{27}/8R_{xy}{}^2R_zN_A$, where R_{xy} and R_z are in Å, and where N_A is Avogadro's number. To reduce artifactual effects that would arise from truncation of interactions at the (arbitrary) location of the finite cell boundaries, the "minimum image" criterion is used to select pairwise interactions between each mobile ion in the cell and all the other ions, some of which may be located in adjacent "image" cells, considered in all Cartesian directions (Allen and Tildesley, 1987). Periodic boundary conditions are imposed at each face of the cell to prevent the depletion of ions as a result of moves outside the cell boundaries (Allen and Tildesley, 1987). The cell is at all times strictly electroneutral and the location of the N-mer (ligand, or complex) is fixed, in order to focus on the thermodynamic consequences of interactions with mobile salt ions in the frame of reference of the dilute, multiply charged species.

The reported results are independent of the initial choices of the number and positions of the ions of the electroneutral salt component. At each MC step, a transition chosen with equal probability from the types described above (moving one or more ions, or inserting/deleting an electroneutral collection of ions) was attempted. Multiple ion moves (Jayaram et al., 1990) ($\lesssim$20 ions), insertions ($\lesssim$16 ions) and deletions ($\lesssim$16 ions) were chosen to optimize acceptance probabilities ($\sim$0.5) and to reduce the computer time required (Olmsted et al., 1991). When attempting ion insertions, locations for inserted ions were chosen

randomly using a distribution that is constant over the cell volume available to the ion centers and 0 elsewhere. When attempting ion moves, trial ion locations (X_t, Y_t, Z_t) were generated from current ion locations (X_c, Y_c, Z_c) using two uniform random variables $0 < \eta_{xy}$, $\eta_z < 1$ according to $X_t = X_c + \eta_{xy}R_{xy}/15$, $Y_t = Y_c + \eta_{xy}R_{xy}/15$ and $Z_t = Z_c + \eta_z R_z/15$ (with the exception that moves resulting in overlap with the volume excluded to ions by the spatially fixed oligoion were not attempted (Olmsted and Hagerman, 1994). More specific details of GCMC transition probabilities for moves of single ions and insertions and deletions of an electroneutral combination of two ions have been provided by Mills et al. (1986) and Jayaram and Beveridge (1991). GCMC transition probabilities for moves involving multiple ions (Jayaram et al., 1990) and insertions and deletions of electroneutral combinations involving ≥2 ions (D. Beveridge, personal communication) are identical to those in Olmsted et al. (1991; Olmsted and Hagerman, 1994).

Equilibration of the simulation consisted of 9×10^4 MC steps, after which $C_{|Z|}(a)$ and C_3 were evaluated from averages over subsequent MC steps, as described below. Reported uncertainties are the standard error of the mean, calculated for block averages. (A block average is the mean of C_3 or $C_{|Z|}(a)$ over 4500 consecutive configurations (Hastings, 1970).) Simulations of LD complexes differ from simulations of N-mers only in that the central 8 charges were eliminated and that in some cases larger values of $|Z_{LD}|$ were simulated. The program was vectorized, including implementation of a vectorized random number generator (Anderson, 1990) to optimize efficiency on a Cray supercomputer.

GCMC determination of surface counterion concentrations

Here we designate by $C_{|Z|}(a)$ the surface counterion concentration associated with a particular axial location on the N-mer ($|Z| = N$), the ligand ($|Z| = 8$) or their complex ($|Z| = N - 8$). More precisely, $C_{|Z|}(a)$ is calculated as the average counterion concentration in the annular volume surrounding the surface of the cylindrical oligoanionic N-mer, oligocationic ligand, or their complex, which extends radially from a to $(a + 1)$ Å and axially over a distance of 1.7 Å and is centered on each of the uniformly spaced monomer units (including, for LD complexes, each of the eight uncharged monomer units). To evaluate $C_{|Z|}(a)$, ion counts at axial positions that are equidistant from the center of the oligomer or complex were pooled. $C_{|Z|}(a)$ was averaged over 10^7 configurations ($C_u = 2.49$ mM: for $N < 50$ cubic cells were used; for $N > 50$, $R_z = R_{xy} + (1.7\ N/2) - 13$ (R_z, R_{xy} in Å)), for which the uncertainties were ≤6%. Each determination of $C_{|Z|}(a)$ required 100–120 min at priority 1 on a Cray Y-MP8/864.

GCMC determination of preferential interaction coefficients

For DNA N-mers, the ligand L^{8+} and central LD complexes, the preferential interaction coefficient $\Gamma_{|Z|,u}$ is evaluated (using Eq. 4) as the slope of a plot of GCMC-determined values of C_3 vs. C_u at fixed $a_\pm$ and T, for C_u sufficiently small so that the plot is linear. Olmsted et al. (1991) describe the criteria used to ensure that an accurate limiting slope of the plot of C_3 vs. C_u is obtained. Six to sixteen evaluations of C_3 were required to obtain acceptably small uncertainties in $\Gamma_{|Z|,u}$ ($8 \le |Z| \le 200$); in general larger numbers of determinations of C_3 were required for smaller N. For all simulations, $C_u \le 1$ mM at $a_\pm = 1.76$ mM and $C_u \le 3$ mM at $a_\pm = 12.3$ mM; R_z/R_{xy} ranged from 1 for small oligoions to 1.6 for $N = 200$. At each $a_\pm$ investigated for the three component solution, the intercept value of C_3 at $C_u = 0$ (designated C_3^o) was estimated from a simulation on the corresponding two component solution containing only salt and solvent in a cubic cell large enough so that C_3^o was not affected by increasing the cell size. Each determination of C_3 was an average over 1.8×10^6 configurations, resulting in uncertainties of $C_3 \le 0.2\%$ (20–50 min at priority 1 on a Cray Y-MP8/864).

The uncertainties in $\Gamma_{|Z|,u}$ for short N-mers (e.g., L^{8+}) are greater in general than those for larger N-mers or LD complexes at the same electrolyte activity. However, the molecule-based preferential interaction coefficient $\Gamma_{|Z|}$, which is required for the evaluation of S_aK_{obs} (via Eq. 6), is the product of $\Gamma_{|Z|,u}$ and $|Z|$. We find that the uncertainty in Γ_8 at $a_\pm = 1.76$ mM is less than the uncertainty in $\Gamma_{|Z|}$ for the longer N-mers and their complexes. At $a_\pm = 12.3$ mM, more computational time was required to reduce the uncertainty of Γ_8 (which is required for all determinations of S_aK_{obs}) so that it did not make the largest contribution to the uncertainty in S_aK_{obs}. The approach adopted was to determine C_3 from two separate simulations (with different initial configurations) for each value of C_u. A total of 17 different values of C_u were investigated.

RESULTS AND DISCUSSION

A molecular view of ion exchange accompanying central binding of L^{8+} to model DNA oligomers

For sufficiently long model DNA N-mers ($|Z| = N$), the axial profile of the surface cation (e.g., Na^+) concentration, $C_N(a)$, is approximately trapezoidal (Olmsted et al., 1989). An interior region, in which $C_N(a)$ exhibits its characteristic polyelectrolyte value ($C_\infty(a) \cong 1.8$ M for model B-DNA at $a_\pm = 1.76$ mM) is flanked by two symmetric terminal regions in which C_N(a) increases monotonically from either end of the oligomer toward the interior (Olmsted et al., 1989). At $a_\pm = 1.76$ mM, the terminal regions each span ~20 charges, corresponding to ~10 bp, over which $C_N(a)$ increases (nearly) linearly from <0.3 M to $C_\infty(a)$. Preliminary GCMC results at higher $a_\pm$ and also lower axial charge density (Olmsted, 1991) as well as PB calculations (J. P. Bond, unpublished observations) indicate that the length of the terminal region of model B-DNA decreases slowly with increasing $a_\pm$ in the experimental range, and that the terminal regions of model denatured (single-stranded) DNA span fewer axial charges (but a greater length) than for native B-DNA. At $a_\pm = 1.76$ mM, model B-DNA oligomers shorter than ~22 bp ($N = 44$) lack an interior region characterized by the polyelectrolyte $C_\infty(a)$ (Olmsted et al., 1989, and unpublished observations). The predicted reduction in $C_N(a)$ at small N is qualitatively in agreement with the ~50% reduction in the enhancement (with respect to pure salt solutions) of ^{23}Na-NMR relaxation rates for a salt-free solution of a 20-bp DNA oligomer, as compared to 160 bp or polymeric DNA (Stein et al., 1995).

At $a_\pm = 1.76$ mM, axial profiles of surface counterion concentrations $C_N(a)$ of some oligomers that are investigated in the present study are shown in Fig. 1, replotted from the data of Olmsted et al. (1989). In particular, the axial profile of the 8-mer represents either the surface cation (Na^+) concentration for a 8-phosphate model DNA oligomer or the surface anion (Cl^-) concentration for the model L^{8+} ligand. For both model 8-mers, the surface concentration of counterions is predicted to be relatively small and only slightly dependent upon axial location (ranging from ~0.06 M at the termini to ~0.07 M in the center). These local concentrations at the surface of an 8-mer far exceed the "bulk" salt concentration (here $C_3^o = 1.83$ mM), but are themselves much lower than the

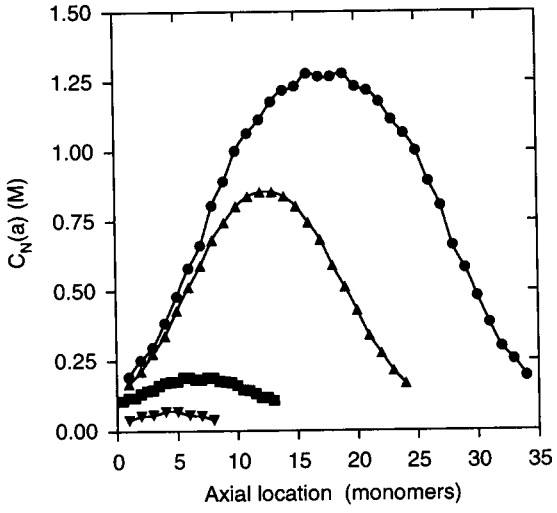

FIGURE 1 GCMC predictions (at $a_{\pm}$ = 1.76 mM) of surface counterion (e.g., Na^+) concentrations $C_N(a)$ (defined in text) as a function of axial location (in monomer units, where 1 is the location of a terminal charge) along cylindrical models of short DNA oligomers. (N = 8 (▼), 13 (■), 24 (▲), 34 (●).) The N = 8 profile also represents the surface concentration of Cl^- along the L^{8+} ligand.

counterion concentrations at the surface of longer oligomers, as illustrated in Fig. 1.

For all of the model LD complexes considered here, neutralization of the central eight charges by the binding of L^{8+} is predicted to result in a dramatic reduction of the surface cation concentration both in and beyond the axial location of the bound site (Fig. 2). GCMC-simulated axial profiles of surface cation concentrations surrounding LD complexes (designated $C_{N-8}(a)$) predict for sufficiently small N a significant reduction in $C_{N-8}(a)$ over the entire length of the N-mer (Fig. 2 *A*; N = 24), or at least into the terminal regions (Fig. 2 *B*; N = 72), so that no polyelectrolyte-like interior region remains.

For two representative longer oligomers (N = 110, 250; Fig. 2 *C*), central binding of L^{8+} is predicted to introduce axial gradients in $C_{N-8}(a)$ extending approximately 20–25 charges in each direction from the center of the neutralized region. Fig. 2 *C* predicts that the binding of L^{8+} to the center of an N-mer for which $N \gtrsim 110$ is qualitatively analogous to dividing the N-mer into two separate (N-8)/2-mers, each long enough to contain an interior region in which $C_N(a)$ exhibits its characteristic polyelectrolyte value. Qualitatively, the axial profile of $C_{N-8}(a)$ for an LD complex provides one molecular-level illustration of the ion exchange component of binding an oligocation (L^{8+}) to an oligoanion (B-DNA N-mer) in a salt solution. In principle, ^{23}Na-NMR experiments may be used to test refined predictions of average surface Na^+ concentrations for specific N-mer sequences (Stein et al., 1995; Braunlin, 1995), and specific ligand-N-mer complexes. Some experimentally accessible thermodynamic consequences of ion redistribution are analyzed in the next sections using preferential interaction coefficients.

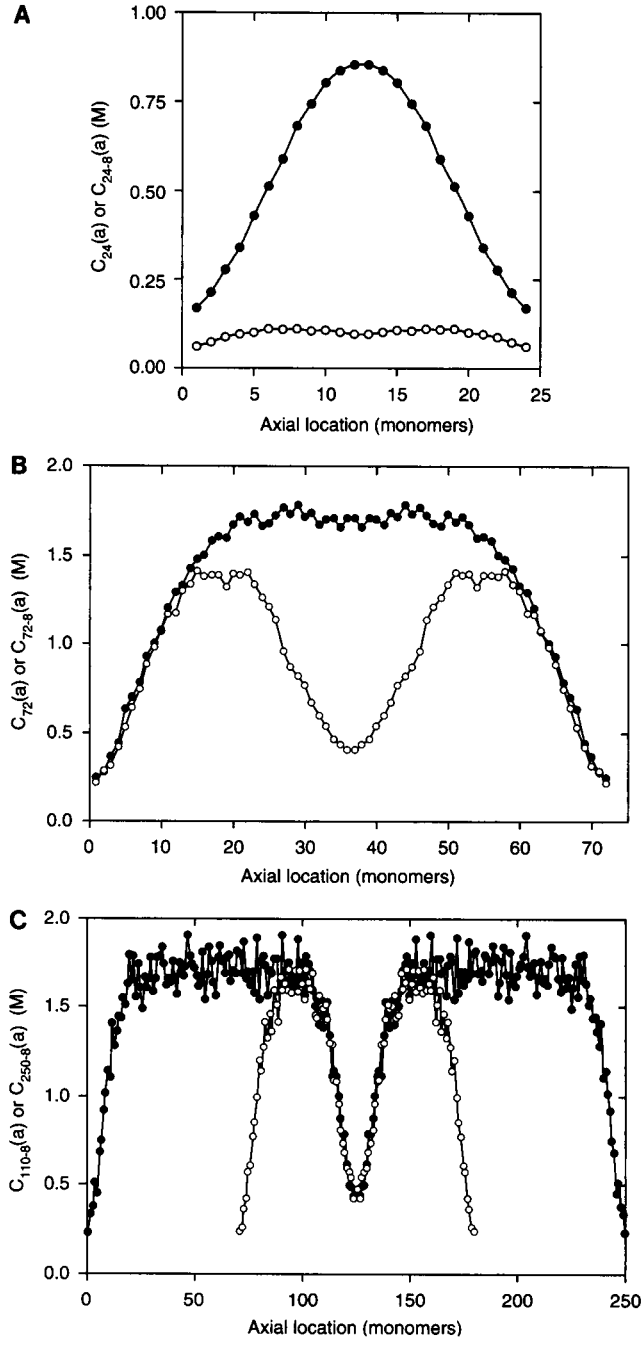

FIGURE 2 GCMC predictions of surface counterion concentration $C_{|Z|}(a)$ as a function of axial location (in monomer units) along cylindrical models of uncomplexed and complexed DNA oligomers, the latter with 8 central charges eliminated to simulate binding of the octacation L^{8+}. (*A*) 24-mer: ●, uncomplexed ($|Z|$ = 24); ○, complexed ($|Z|$ = 24–8); (*B*) 72-mer: ●, uncomplexed ($|Z|$ = 72); ○, complexed ($|Z|$ = 72–8); (*C*) central complexes of L^{8+} with 110-mer (○) and 250-mer (●). (In *A*, *B*, and for the 250-mer *C*, the axial location of the terminal charge is at 1; for the 110-mer in *C* the axial location of the terminal charge is at 71. Both oligomers in *C* are centered at axial location 125.5.)

Figs. 1 and 2 illustrate two essential qualitative features of the redistribution in the local surface counterion concentrations that arise from oligocation-oligoanion binding: 1) the "end effects" on $C_{N-8}(a)$ in the vicinity of the bound L^{8+}; and

2) the interplay between these L^{8+}-induced end-effects and the preexisting coulombic end-effects on $C_N(a)$ of the free DNA N-mer, which together determine the extent of reduction of the average $C_N(a)$ that results from the binding of L^{8+}. These oligoelectrolyte effects are expected to be general insofar as they are attributable to coulombic interactions, whose range is long enough so that the underlying cylindrical symmetry of the system predominates. However, our GCMC predictions of $C_{|Z|}(a)$ are not expected to provide more than an estimate of the average counterion concentration near the surface of a real DNA oligomer or its complex, because of the various idealizations of our model. Details of the local charge distribution and local geometry of the DNA surface and, in solution, fluctuations of these quantities due to local diffusional motions, certainly would affect in particular axial and angular variations of local ion distributions in the near vicinity of a nucleic acid. Information sufficient to permit a unique and verifiable parameterization of these details is rarely available. Fortunately, there is at present no clear indication that a description more refined than that specified by the standard model assumptions is required to obtain sufficiently accurate predictions of the thermodynamic coefficients that are of interest in the following sections.

GCMC predictions of preferential interaction coefficients for uncomplexed oligoelectrolytes (B-DNA *N*-mers, L^{8+})

Preferential interaction coefficients ($\Gamma_{N,u}$) expressed per oligoion charge were predicted for cylindrical models of oligomeric B-DNA with different numbers of charges ($|Z_D| = N$; $8 \leq N \leq 100$) in the salt activity range $a_\pm = 1.76$–12.3 mM from GCMC determinations of C_3 as a function of C_u. Representative plots of C_3 vs. C_u for $N = 24$ and $N = 72$ at $a_\pm = 1.76$ mM are shown in Fig. 3, *A* and *B*, respectively. The preferential interaction coefficient $\Gamma_{N,u}$, evaluated as the slope of a plot of C_3 vs. C_u (cf. Eq. 4), is determined by linear regression. The resulting intercept with the C_3 axis is in all cases found to be independent of the length of the oligoion simulated (cf. Fig. 3) and equal to the concentration of salt at $a_\pm = 1.76$ mM obtained independently by GCMC simulations in the absence of the oligoion ($C_3^\circ = 1.834 \pm 0.001$ mM). This correspondence indicates that $\Gamma_{N,u}$ has been correctly determined in the context of the GCMC analysis of the standard primitive model of the oligoelectrolyte solution. Because the preferential interaction coefficient of L^{8+} ($\Gamma_{8,u}$, which for the model assumptions adopted here is identical to that of a B-DNA 8-mer) is used in each calculation of $S_a K_{obs}$ at the corresponding salt activity, and because the statistical uncertainty in the estimation of $\Gamma_{N,u}$ is largest for small N, additional simulations were required to evaluate this coefficient (cf. Methods and Fig. 4). Fig. 4, in which the quantity C_3-C_3° is plotted vs. C_u in order to represent data from two different salt concentrations on one graph, shows the GCMC evaluations of $\Gamma_{8,u}$ at $a_\pm = 1.76$ and $a_\pm = 12.3$ mM. The complete set of $\Gamma_{N,u}$ at 1.76, 7.07 and 12.3 mM is tabulated in Table 1.

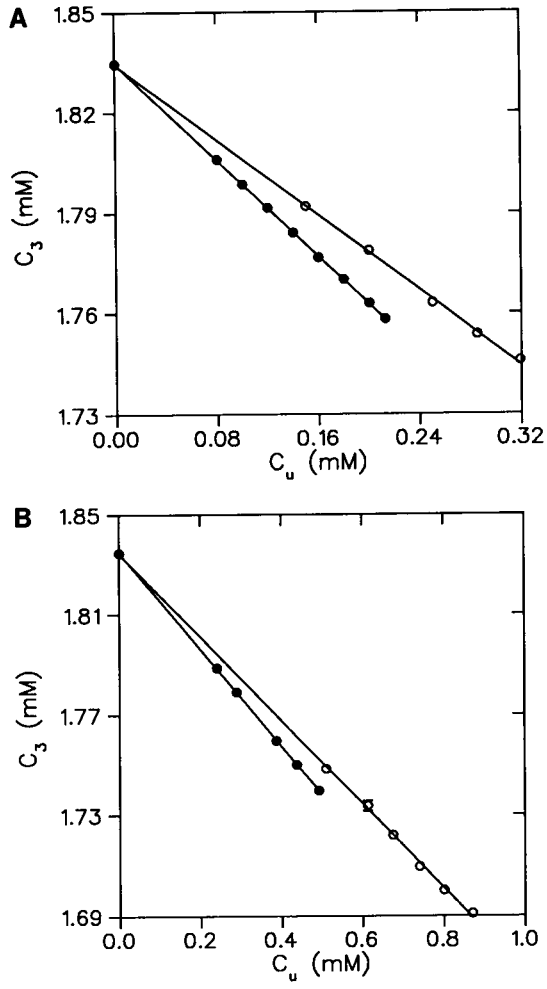

FIGURE 3 Pairs of GCMC predictions of $\Gamma_{|ZJ|,u}$, the per-charge preferential interaction coefficients of DNA oligomers and of the corresponding central LD complexes, from C_3 vs. C_u plots at $a_\pm = 1.76$ mM. (*A*) 24-mer (○) and corresponding ($|Z_{LD}| = 24$–8) central complex (●); (*B*) 72-mer (○) and corresponding ($|Z_{LD}| = 72$–8) central complex (●). The solid lines were obtained by linear regression of C_3 on C_u.

From Table 1, it is apparent that $\Gamma_{N,u}$ depends on both N and $a_\pm$. The observation (at any fixed $a_\pm$) that $-\Gamma_{N,u}$ decreases as N increases demonstrates the increase in nonideality (per charge) with increasing N that accompanies the increase in average local cation concentration ($\bar{C}_N(a)$) and that signals the approach to polyelectrolyte behavior of the N-mers. Data for long oligoelectrolytes ($N \geq 24$), for which $\Gamma_{N,u}$ approaches the polymer limit as a linear function of N^{-1} (cf. Eq. 5; Olmsted et al., 1989, 1991), are plotted in Fig. 5. Of fundamental significance is the prediction that the slope α of the plot of $-\Gamma_{N,u}$ vs. N^{-1} decreases with increasing $a_\pm$ in the range examined, so that the linear plots share a common point of intersection in the vicinity of $N = 48$. Fig. 5 illustrates the gradual transition from the thermodynamic behavior of ordinary electrolyte solutions to that of

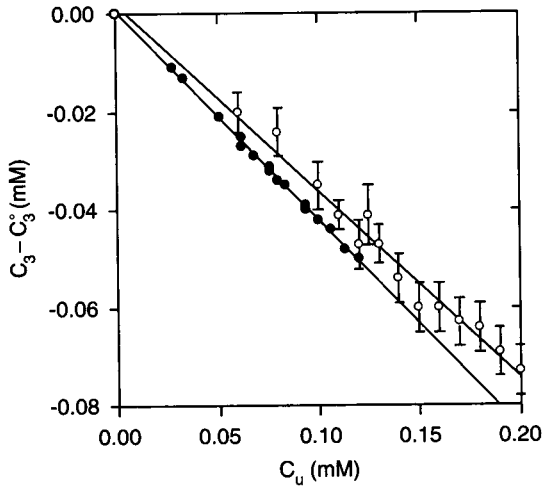

FIGURE 4 GCMC predictions of $\Gamma_{8,u}$, the per-charge preferential interaction coefficient of a model B-DNA 8-mer and of the model ligand L^{8+}. GCMC values of C_3, expressed as the difference $C_3 - C_3^\circ$, are plotted vs. oligoion monomer concentration C_u for two values of the electrolyte activity: $a_\pm$ = 1.76 mM (●); $a_\pm$ = 12.3 mM (○). In each case, C_3° is the independently determined (GCMC) salt concentration at that $a_\pm$ in the absence of the oligoion. The solid lines were obtained by linear regression of $C_3 - C_3^\circ$ on C_u.

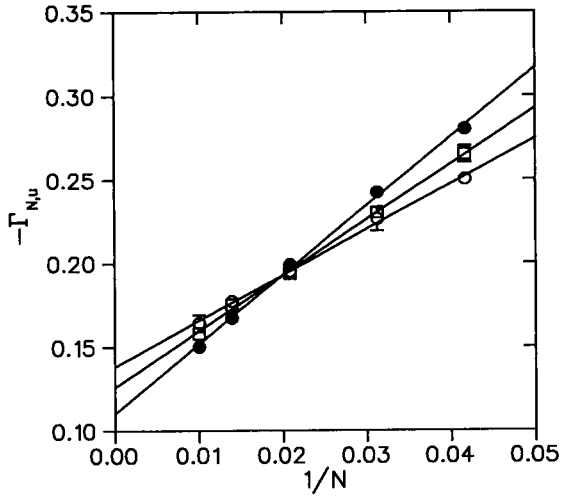

FIGURE 5 GCMC predictions of the per-charge preferential interaction coefficient of model B-DNA oligomers in univalent salt ($\Gamma_{N,u}$; $|Z_D| = N$), as a function of $1/N$ at three salt activities: $a_\pm$ = 1.76 mM (●), $a_\pm$ = 7.07 mM (□), $a_\pm$ = 12.3 mM (○). The solid lines were obtained by linear regression of $\Gamma_{N,u}$ on $1/N$ at each salt activity.

TABLE 1 Model B-DNA oligoelectrolytes (*N*-mers; $|Z_D| = N$): predicted dependence of $-\Gamma_{N,u}$ on N and on $a_\pm$

	$-\Gamma_{N,u}$		
N	$a_\pm$ = 1.76 mM (C_3° = 1.834 ± 0.001 mM)	$a_\pm$ = 7.07 mM (C_3° = 7.661 ± 0.001 mM)	$a_\pm$ = 12.3 mM (C_3° = 13.500 ± 0.004 mM)
8	0.424 ± 0.004		0.375 ± 0.025
10	0.405 ± 0.004	0.388 ± 0.010	
14	0.363 ± 0.003	0.339 ± 0.003	
16	0.340 ± 0.002	0.309 ± 0.006	
24	0.280 ± 0.002	0.265 ± 0.005	0.250 ± 0.005
32	0.242 ± 0.001	0.230 ± 0.002	0.226 ± 0.007
34	0.231 ± 0.001		
48	0.199 ± 0.002	0.194 ± 0.002	0.195 ± 0.004
72	0.167 ± 0.002	0.175 ± 0.001	0.177 ± 0.003
100	0.150 ± 0.002	0.158 ± 0.002	0.164 ± 0.005

polyelectrolyte-electrolyte solutions. As will be discussed below, Fig. 5 has implications that are of particular relevance to the interpretation of $S_a K_{obs}$ as a composite measure of the effect of variations in salt activity on the binding of a short oligocation to a long oligoanion.

In the polyelectrolyte limit ($N \rightarrow \infty$), the contributions to nonideality arising from interactions between salt and the N-mer ($\Gamma_{N,u}$) decrease as $a_\pm$ increases. At a molecular level, this thermodynamic behavior results from the buffering of the local cation concentration against changes in the bulk salt concentration, so that the ratio of local to bulk cation concentrations decreases with increasing salt concentration. Fig. 5 predicts that N-mers with $N \gtrsim 48$ will exhibit the polyelectrolyte-like direction of change of $\Gamma_{N,u}$ with $a_\pm$. (Note that these longer N-mers ($N \gtrsim 48$) also all exhibit a polyelectrolyte-like interior region (Olmsted et al., 1989).)

On the other hand, application of Debye-Hückel theory to short N-mers leads to the prediction that $\Gamma_{N,u}$, which characterizes electrolyte-N-mer preferential interactions, increases with increasing $a_\pm$ (Olmsted, 1991), in parallel with the increase in the nonideality of a simple electrolyte solution with increasing $a_\pm$ over this range. Fig. 5 predicts that N-mers with $N \lesssim 48$, which lack a significant polyelectrolyte-like interior region, will exhibit the same direction of change of $\Gamma_{N,u}$ with increasing $a_\pm$ as that characteristic of ordinary electrolytes.

At a given salt concentration the thermodynamic consequences of the electrolyte ion gradients surrounding an N-mer, described by Γ_N or $\Gamma_{N,u}$, are formally the same as if the counterions of the N-mer were incompletely dissociated (i.e., a weak electrolyte) (Anderson and Record, 1982, 1993; Record and Richey, 1988; Record and Anderson, 1995). In this thermodynamic (but not molecular) interpretation of Γ_N, the quantity $(N + 2\Gamma_N)$ (cf. Eq. 6) is the number of counterions associated with the N-mer, and $(1 + 2\Gamma_{N,u})$ is the fraction of a counterion associated per structural charge on the N-mer (cf. commentary following Eq. 6 above). Specifically, for DNA N-mers in NaCl solutions, $(1 + 2\Gamma_{N,u})$ is the thermodynamic extent of association (i.e. thermodynamic binding) of Na^+ per DNA phosphate. Table 1 and Fig. 5 predict that the thermodynamic binding of Na^+ per DNA charge increases with increasing N. The limiting values of $(1 + 2\Gamma_{N,u})$ at low $a_\pm$ for simple electrolytes and polymeric B-DNA are 0 and 0.88, respectively (Anderson and Record, 1983). At $a_\pm$ = 1.76 mM, $(1 + 2\Gamma_{N,u})$ increases from 0.152 ± 0.008 for N = 8 to 0.700 ± 0.004 for N = 100. For $N < 48$, thermodynamic binding of counterions per oligoion charge increases with increasing $a_\pm$. For $N > 48$, thermodynamic binding of counterions per oligoion charge actually decreases with increasing $a_\pm$. This latter, purely coulombic result is a clear indication that in

the present context thermodynamic binding cannot usefully be described as a mass-action phenomenon, and that its dependence on $a_\pm$ should not be interpreted in terms of site binding. To date NMR measurements yield no indication of any site binding of Na^+ to DNA phosphates in dilute aqueous solution (cf. Braunlin, 1995 and refs. therein).

GCMC predictions of preferential interaction coefficients of octacation (L^{8+})-B-DNA central complexes

Preferential interaction coefficients ($\Gamma_{|Z_{LD}|,u}$), expressed per unneutralized charge on the LD complex, were calculated at $a_\pm = 1.76$ mM and $a_\pm = 12.3$ mM for cylindrical models of L^{8+}-N-mer central complexes from GCMC predictions of C_3 as a function of C_u. Representative plots of C_3 vs. C_u are shown in Fig. 3. The extrapolated value of C_3 at $C_u = 0$ is within statistical uncertainty of the GCMC prediction (C_3^o) for a salt solution containing no oligomer at the same $a_\pm$ and T. Results of these simulations are listed in Table 2. The dependence of $\Gamma_{|Z_{LD}|,u}$ on N and on $a_\pm$ are qualitatively the same as for the case of uncomplexed oligoions (cf. Table 1 and the preceding section). At both values of $a_\pm$ investigated, $-\Gamma_{|Z_{LD}|,u}$ decreases as N increases. For $N \leq 48$, $-\Gamma_{|Z_{LD}|,u}$ decreases as $a_\pm$ increases, but for $N \geq 72$, $-\Gamma_{|Z_{LD}|,u}$ increases as $a_\pm$ increases.

Prediction of S_aK_{obs} as a function of N from preferential interaction coefficients

GCMC preferential interaction coefficients for L, D and LD as functions of N at $a_\pm = 1.76$ mM and $a_\pm = 12.3$ mM (Tables 1 and 2) were used to predict S_aK_{obs} and, in accordance with Eq. 6, contributions to S_aK_{obs} attributable to anion release from the ligand and to cation release from the DNA upon complexation. Table 3 lists these contributions together with predicted values of S_aK_{obs}, which also are plotted as a function of N in Fig. 6.

Fig. 6 illustrates the novel (and to date untested) prediction of this computational thermodynamic study that S_aK_{obs} for central binding of an oligocation to an oligonucleotide (N-mer) is a strong function of N. For $N = 200$, the average value of S_aK_{obs} for the range of $a_\pm$ examined is 7.2 ± 1.3, assuming that any variation of S_aK_{obs} with $a_\pm$ in this range (cf. Table 3) is negligible compared with statistical error. As N decreases from 200, $|S_aK_{obs}|$ appears to increase to a maximum at $N \approx 72$ (cf. Table 3 and Fig. 6). Detailed examination of the thermodynamic basis for this maximum is deferred to a subsequent paper in which binding of L^{8+} to polymeric DNA is analyzed (Bond et al., manuscript in preparation). To test whether the apparent increase in S_aK_{obs} as N decreases from 200 to 72 could be an artifact of the statistical uncertainty in the estimates of the preferential interaction coefficients, we performed a weighted fitting of $|S_aK_{obs}|$ for $N \geq 72$ at $a_\pm = 1.76$ mM and $a_\pm = 12.3$ mM to a single straight line, and found that with >99.9% confidence the slope is less than 0. As N decreases from 72, $|S_aK_{obs}|$ decreases dramatically (cf. Table 3 and Fig. 6). For the association of L^{8+} with 8-mer DNA, the effect of salt concentration on K_{obs}, as characterized by S_aK_{obs}, is predicted to be only 25–40% as large as for the association of L^{8+} with 72-mer DNA. This result is reasonable; the Debye-Hückel prediction for the effect of salt concentration on K_{obs} for any equilibrium involving spherical ions ($|Z_j| = 1, 2$) is far smaller in magnitude (and of a different functional form) from that predicted here.

Table 3 and Eq. 6 provide a thermodynamic basis for understanding the strikingly large variation in S_aK_{obs} with N shown in Fig. 6. The thermodynamic quantity $-S_aK_{obs}$ may be interpreted as the stoichiometry of ion release in the complexation process. This concept may be appreciated by considering the simple case of the binding of L^{8+} to an 8-mer. At $a_\pm = 1.76$ mM, from Table 1, the GCMC-predicted preferential interaction coefficient is $\Gamma_{8,u} = -0.424 \pm 0.004$, and the predicted amounts of thermodynamic binding of counterions to L^{8+} and to the 8-mer are both $8 + 2\Gamma_8 = 8(1 + 2\Gamma_{8,u}) = 1.22 \pm 0.03$. L^{8+} is predicted to behave thermodynamically as a "weak" oligoelectrolyte with 1.22 ± 0.03 associated Cl^- at $a_\pm = 1.76$ mM; the DNA 8-mer is also predicted to behave thermodynamically as a "weak" oligoelectrolyte, with 1.22 ± 0.03 associated Na^+ at $a_\pm = 1.76$ mM. At $a_\pm = 12.3$ mM, from Table 1, $\Gamma_{8,u} = -0.375 \pm 0.025$ and $8(1 + 2\Gamma_{8,u}) = 2.0 \pm 0.2$, so the GCMC-predicted amounts of thermodynamic binding of counterions to L^{8+} and to the 8-mer are significantly larger than at $a_\pm = 1.76$ mM. The complexation of L^{8+} with the 8-mer produces an uncharged LD complex, which does not interact coulombically with the electrolyte and hence has no thermodynamically bound counterions. Consequently the complexation of L^{8+} and a DNA 8-mer is predicted to release $2(1.22 \pm 0.03) = 2.4 \pm 0.1$ ions at $a_\pm = 1.76$ mM, and to release 4.0 ± 0.4 ions at $a_\pm = 12.3$ mM. This novel thermodynamic prediction is not a mere consequence of the electroneutrality constraint or of the definitions of electroneutral thermodynamic components (Anderson and Record, 1993).

With increasing N, the amount of cation association with both the uncomplexed and complexed forms of the N-mer is predicted to increase. The difference between these two

TABLE 2 Model B-DNA N-mer-L^{8+} complexes ($|Z_{LD}| = N - 8$): predicted dependence of $-\Gamma_{|Z_{LD}|,u}$ on N and on $a_\pm$

N	$\lvert Z_{LD}\rvert$	$-\Gamma_{\lvert Z_{LD}\rvert,u}$	
		$a_\pm = 1.76$ mM	$a_\pm = 12.3$ mM
24	16	0.359 ± 0.003	0.328 ± 0.007
32	24	0.306 ± 0.002	0.287 ± 0.008
34	26	0.292 ± 0.002	
48	40	0.236 ± 0.002	0.230 ± 0.004
72	64	0.193 ± 0.002	0.199 ± 0.005
100	92	0.162 ± 0.002	0.178 ± 0.005
150	142	0.142 ± 0.001	
176	168	0.132 ± 0.001	
200	192	0.128 ± 0.001	0.152 ± 0.004

TABLE 3 Predicted dependence of S_aK_{obs} for binding of L^{8+} to DNA *N*-mers; contributions to $-S_aK_{obs}$ from the *N*-mer, L^{8+}, and complex

DNA oligomer size (N)	$a_\pm$ = 1.76 mM				$a_\pm$ = 12.3 mM			
	Total ion association ($\lvert Z_j \rvert + 2\Gamma_{\lvert Z_j \rvert}$)*			Ion release‡	Total ion association ($\lvert Z_j \rvert + 2\Gamma_{\lvert Z_j \rvert}$)*			Ion release‡
	N-mer	L^{8+}	Complex	($-\Delta(\lvert Z_j \rvert + 2\Gamma_{\lvert Z_j \rvert} = -S_aK_{obs}$)	N-mer	L^{8+}	Complex	($-\Delta(\lvert Z_j \rvert + 2\Gamma_{\lvert Z_j \rvert} = -S_aK_{obs}$)
8	1.22 ± 0.03	1.22 ± 0.03	0	2.4 ± 0.1	2.0 ± 0.2	2.0 ± 0.2	0	4.0 ± 0.4
24	10.4 ± 0.1	1.22 ± 0.03	4.5 ± 0.1	7.1 ± 0.1	12.0 ± 0.2	2.0 ± 0.2	5.5 ± 0.2	8.5 ± 0.4
32	16.6 ± 0.1	1.22 ± 0.03	9.3 ± 0.1	8.5 ± 0.2	17.5 ± 0.4	2.0 ± 0.2	10.2 ± 0.4	9.3 ± 0.6
34	18.3 ± 0.1	1.22 ± 0.03	10.8 ± 0.1	8.7 ± 0.2				
48	28.9 ± 0.2	1.22 ± 0.03	21.1 ± 0.1	9.0 ± 0.3	29.3 ± 0.4	2.0 ± 0.2	21.6 ± 0.3	9.7 ± 0.5
72	48.3 ± 0.3	1.22 ± 0.03	39.3 ± 0.2	10.2 ± 0.4	46.5 ± 0.4	2.0 ± 0.2	38.5 ± 0.7	10.0 ± 0.8
100	70.3 ± 0.4	1.22 ± 0.03	62.2 ± 0.4	9.3 ± 0.5	67.2 ± 1.0	2.0 ± 0.2	59.3 ± 0.9	10.0 ± 1.3
150	109.5 ± 0.7§	1.22 ± 0.03	101.8 ± 0.3	8.9 ± 0.8				
176	129.9 ± 0.8§	1.22 ± 0.03	123.5 ± 0.3	7.6 ± 0.9				
200	148.8 ± 0.9§	1.22 ± 0.03	142.7 ± 0.5	7.3 ± 1.0	139.0 ± 0.8§	2.0 ± 0.2	133.6 ± 1.5	7.4 ± 1.7

*"Ion association" refers to the thermodynamic association of cations with an oligoanion (or of anions with an oligocation).
‡"Ion release" refers to the reduction in the extent of thermodynamic association upon complexation.
§Estimated by linear extrapolation of the data given in Table 1 using Eq. 5.

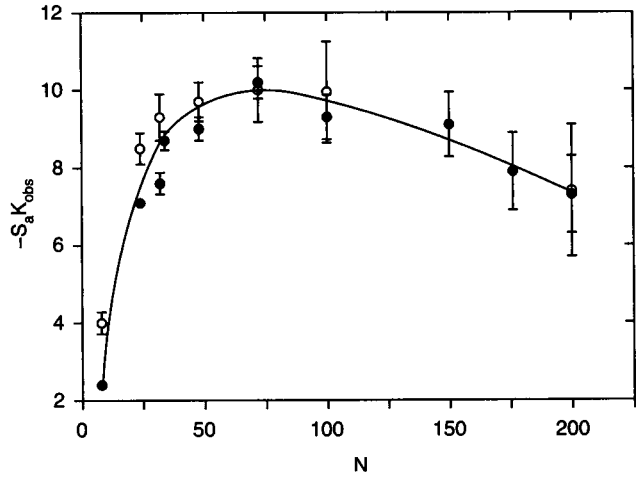

FIGURE 6 GCMC predictions of $-S_aK_{obs}$, the experimentally accessible salt derivative of K_{obs}, interpreted as the net thermodynamic stoichiometry of participation of salt ions, for binding of an 8-mer ligand (L^{8+}) to model DNA *N*-mers as a function of *N* at two salt activities $a_\pm$: $a_\pm$ = 1.76 mM (●), $a_\pm$ = 12.3 mM (○). The solid line was drawn to guide the eye.

quantities is the amount of cation release from the *N*-mer upon binding L^{8+}. The results in Table 3 indicate that the amount of cation release at $a_\pm$ = 1.76 mM increases from 1.22 ± 0.03 for N = 8 to 7.5 ± 0.2 for N = 34 and attains a maximum of 9.0 ± 0.4 for N = 72. For N = 200, the amount of cation release is 6.1 ± 1.0. Thus, cation release is predicted to contribute 50% of the ion release for N = 8, increasing to a maximum contribution of ~90% for N = 72 and then decreasing to ~80–85% at larger N. By comparison, for binding of L^{8+} to polyelectrolyte ($N \rightarrow \infty$) DNA, application of limiting-law (low salt concentration) thermodynamic expressions from counterion condensation theory of cylindrical polyelectrolytes (Manning, 1969) led Record et al. (1976) to predict a release of 7.0 cations from the polyion (and no anions from the ligand). It is noteworthy that this limiting law result is quite consistent with the predicted values of S_aK_{obs} for large N (N = 176, 200) (Table 3), although at the (finite) salt concentrations covered by our GCMC simulations, the release of cations from the DNA (Eq. 6) is less than the limiting law prediction. Table 3 shows that the smaller cation contribution to S_aK_{obs} is compensated by the larger amount of anion release predicted to occur from L^{8+}. This compensation is expected to be general for binding of small oligocations to large oligoanions, on the basis of Fig. 5, as discussed below.

Although the statistical uncertainty associated with the determinations of S_aK_{obs} and the relatively narrow range of $a_\pm$ investigated to date prevent precise conclusions about the sensitivity of S_aK_{obs} to changes in $a_\pm$, Table 3 and Fig. 6 predict that, at least for $N \geq 72$, S_aK_{obs} is relatively insensitive to changes in $a_\pm$, as has been observed experimentally (at salt activities generally higher than those examined here) for the binding of oligocationic ligands to polymeric DNA (cf. Lohman and Mascotti, 1992 for a review). However, the contributions to S_aK_{obs} arising from L^{8+}, the *N*-mer, and the LD complex individually vary with $a_\pm$ (cf. Table 3 and Fig. 5), so that the near-constancy of S_aK_{obs} at large enough N is predicted to result from compensating changes in these contributions with changes in $a_\pm$. The total ion association with L^{8+} (given by $8 + 2\Gamma_{8,u}$; cf. Eq. 6) increases from 1.22 ± 0.03 to 2.00 ± 0.20 (and thus the contribution to S_aK_{obs} arising from ion release from L^{8+} becomes more negative) as $a_\pm$ increases from $a_\pm$ = 1.76 mM to $a_\pm$ = 12.3 mM (Table 3). At least for $N \geq 72$, the total extents of ion association with both the uncomplexed and complexed *N*-mers ($(\lvert Z_D \rvert + 2\Gamma_{\lvert Z_D \rvert})$ and $(\lvert Z_{LD} \rvert + 2\Gamma_{\lvert Z_{LD} \rvert})$, respectively) decrease with increasing $a_\pm$, and the contribution to S_aK_{obs} made by ion release from the *N*-mer upon complexation appears to become less negative with increasing $a_\pm$.

CONCLUDING DISCUSSION

The profile of the electrostatic potential along the surface and parallel to the axis of a cylindrical (or at least approximately

rod-like) charged N-mer obviously must diminish in magnitude sufficiently near either end of the N-mer. This effect must be present even for large N (i.e., for a polymer), but detecting it via any measurable macroscopic property becomes progressively more difficult as N increases. Determining how a given measurable property of an N-mer approaches the value characteristic of the corresponding polymer as a function of N is essential to compare results obtained for different oligomers and to extrapolate to the polymeric case quantitative measurements on oligomers. In particular, because oligonucleotides are frequently used in biophysical studies of conformational transitions and ligand binding equilibria, it is necessary to understand coulombic end effects to make quantitative comparisons of binding constants at fixed salt concentration, as well as of the effects of salt concentration on these equilibria and those obtained or anticipated for polymeric nucleic acids.

Summary of previous theoretical work on charged cylindrical oligomers

Elson et al. (1970) apparently were the first to quantify an oligoelectrolyte end effect on a measurable property of cylindrical oligomers. Specifically, they determined experimentally the dependence on N ($8 < N < 22$) of the derivative $dT_m/d\ln[M^+]$, where T_m is the temperature of the midpoint of the "melting" conformational transition of a series of d(TA) oligomers and M^+ is the concentration of univalent cations in the solution. Elson et al. recognized that the observed N-dependence of $dT_m/d\ln[M^+]$ is attributable to long range electrostatic interactions, and they obtained quantitative fittings of their results by summations of screened coulombic potentials according to the method of Schildkraut and Lifson (1965).

The results of Elson et al. imply that $dT_m/d\ln[M^+]$ approaches, as a linear function of $1/N$, the limiting value characteristic of the corresponding polymeric conformational transition. This characteristic functional form for an end-effect was recognized by Record and Lohman (1978), who analyzed it in terms of a two-regime (interior, end) model adapting concepts from Manning's counterion condensation theory (1969). Although the quantitative details of this analysis have been superseded by our later results based on GCMC simulations (Olmsted et al., 1991), the study by Record and Lohman provided the first theoretical explanation for the specific N^{-1}-dependence of a thermodynamic property of charged cylindrical oligomers, and provided the first (lower bound) estimate of the axial range of the oligo- end effect on the local counterion concentration at the surface of a nucleic acid oligomer.

The axial variation of the electrostatic potential along the surface of cylindrical oligomers (of two charge densities, both substantially lower than that of B-DNA) was investigated by Katoh and Ohtsuki (1982) by means of numerical solutions of a cylindrically symmetric two-dimensional PB equation. Although reported exclusively in terms of the PB potential, these results are effectively equivalent to an illustration of an oligoelectrolyte end effect on the axial profile of the local counterion concentration as a function of position along the surface of a cylindrically symmetric oligomer. Katoh and Ohtsuki investigated the effects of different dielectric constants and salt concentrations on the predicted electrostatic potential contours, but did not examine how (or whether) they depend on N.

For a detailed structural model of an oligomer of B-DNA ($N = 60, 80$) Klein and Pack (1983) used numerical solutions of a three-dimensional form of the PB equation to predict axial profiles of the "average charge density" (integrated out to 60 Å from the van der Waals contact surface) at two salt concentrations (10^{-5} and 10^{-2} M). Their objective was to determine whether the mobile ion charge distribution surrounding a segment composed of 20 bases situated at the center of a 60-mer can be taken as representative of the interior of the corresponding polymer. At 10^{-2} M they found for both oligomers that the "average charge density" varies significantly over the first 10–20 bases from either end before reaching a common plateau, which presumably would also be observed for any longer oligomer of the same structure. This finding is in qualitative agreement with the characteristics of the axial profiles of counterion surface concentrations reported here. At the much lower salt concentration (10^{-5} M), the axial profiles of "average charge densities" obtained by Klein and Pack differ at all comparable positions along the two oligomers, so that apparently neither contains any region exhibiting the same "average charge density" as would surround an internal segment of the corresponding polymer.

Olmsted et al. (1989, 1991) were the first to use GCMC simulations to quantify oligoelectrolyte end effects on average molecular and thermodynamic properties of cylindrical DNA oligomers. Both the axial average of the local concentration of univalent cations at the surface of the charged cylinder $\bar{C}_{|Z|}(a)$ and the preferential interaction coefficient expressed per oligomer charge $\Gamma_{3uJ} \equiv \Gamma_{32J}/|Z_J|$ were predicted to approach their respective polymeric values as linear functions of the reciprocal of the degree of polymerization N (or equivalently of $|Z|$) of the oligomer (Olmsted et al., 1989, 1991). They also quantified the onset of the polyelectrolyte character of both molecular and thermodynamic properties, for example by determining the range of lengths over which DNA oligomers lack any central region in which the surface cation concentration is as large as that in polyelectrolyte DNA (Olmsted et al., 1989).

Recently, after the simulations reported here were completed, Misra et al. (1994) published PB calculations of the effect of salt concentration on the binding of one monovalent and two divalent cations (antibiotics) to the center of B-DNA oligomers. These calculations incorporate all-atom models for the B-DNA and for the antibiotics. The solvent was treated as a continuum, but variations in the dielectric constant of the solution were taken into account. The thermodynamic analysis was explicitly based not on preferential

interaction coefficients but on contributions to the electrostatic free energy and the derivatives of contributions to the electrostatic free energy with respect to salt concentration. For the divalent antibiotics, they found S_aK_{obs} approximately -2, independent of salt concentration, and in agreement with their calculation based on a cylindrical model for DNA and for the DNA-divalent cation complex, the latter with two charges neutralized to simulate ligand binding. They found no difference in the predicted value of S_aK_{obs} for binding of a divalent cation to the two DNA oligomers ($N = 24$, $N = 114$). On the basis of the GCMC results reported here, we expect that binding of a divalent cation to N-mers would exhibit a reduction in $|S_aK_{obs}|$ at sufficiently small N. However, for binding of L^{8+}, Fig. 6 shows that S_aK_{obs} at $N = 24$ happens to be within uncertainty of the polymer ($N \to \infty$) result (although a function of $a_\pm$), and that S_aK_{obs} for $N = 114$ is somewhat larger in magnitude than the polymer result (and apparently less dependent on $a_\pm$ than for $N = 24$). Hence, the lack of an effect of N on S_aK_{obs} for binding of L^{2+} found by Misra et al. (1994) may not be representative of all values of N in the oligomeric range.

Predictions of specific DNA conformational features in solution, the solvent distribution, and the proximity of counterions to phosphate oxygens and DNA bases have been obtained from molecular dynamics simulations of oligomeric DNA duplexes (Seibel et al., 1985; van Gunsteren et al., 1986; Swaminathan et al., 1991; Fritsch et al., 1993) and triplexes (Laughton and Neidle, 1992; Mohan et al., 1993). These studies incorporate structural information to obtain an explicit atom representation of the DNA and treat both solvent molecules and counterions explicitly as interacting particles. In each case only one length of the nucleic acid oligomer was investigated. None of these studies using explicit solvent molecules report either preferential interaction coefficients or any axial dependence of counterion concentrations, and none examine ligand-DNA complexes.

Summary of theoretical and experimental implications of the present study

Here we have reported the results of thermodynamically rigorous GCMC simulations for primitive models of solutions containing excess univalent salt ($a_\pm$ = 1.76–12.3 mM) and one of the following species: an octavalent oligocation, L^{8+}; an oligomeric B-DNA N-mer ($8 \le N \le 100$); or a complex (LD) of L^{8+} at the center of an N-mer ($24 \le N \le 250$). At the molecular level our simulations predict that formation of the L^{8+}-N-mer complex, modeled by eliminating the 8 central charges from the N-mer, results in a dramatic reduction in the surface cation concentration over a region of the N-mer including but extending well beyond the location of the neutralized charges. Anion accumulation near L^{8+} is completely eliminated upon binding L^{8+} to B-DNA, but this effect is minor relative to the reduction in accumulated cations near the B-DNA upon binding L^{8+}. For $N \le 72$, the neutralization of 8 central charges affects the entire axial profile of the surface cation concentration, or at least extends into the terminal regions of the oligomer (Fig. 2). For $N \ge 110$, between the site of complexation and each end of the N-mer, our simulations predict a region that exhibits the polyelectrolyte value of the surface cation concentration (~1.8 M).

At the thermodynamic level, GCMC simulations have been used to characterize the transition of the response of the preferential interaction coefficient of an oligoelectrolyte (N-mer) to changes in $a_\pm$ from that characteristic of simple electrolytes (at small N) to the qualitatively different response characteristic of polyelectrolytes (at large N). We obtain the novel prediction that $-S_aK_{obs}$ for central binding of L^{8+} to cylindrical N-mers varies strongly with N for $N <$ 200. For small enough N, $-S_aK_{obs}$ is predicted to decrease toward the value characteristic of central binding of L^{8+} to polymeric B-DNA in this range of $a_\pm$ (Bond et al., manuscript in preparation). At values of N smaller than that corresponding to the maximum, $-S_aK_{obs}$ is predicted to decrease toward 0, as a consequence of the much smaller amount of ion accumulation near very short uncomplexed oligomers. To the extent that these trends in S_aK_{obs} are governed by long range coulombic interactions, they are expected to be qualitatively the same for any charge on the oligocationic ligand (provided Z_L is sufficiently less than N of the oligomer) and for any more detailed structures of the ligand or of the oligomeric DNA to which it binds.

In this paper the dependence of S_aK_{obs} on N has been emphasized rather than its dependence on $a_\pm$. At the salt activities investigated here (in the range 1.76–12.3 mM), S_aK_{obs} is predicted to be salt-insensitive for the longer N-mers, but only because of compensating changes in the three preferential interaction coefficients pertaining to the participants in the reaction. For the shorter oligomers ($N \lesssim 24$) a significant salt dependence of S_aK_{obs} (corresponding to a nonlinear plot of $\ln K_{obs}$ vs. $\ln a_\pm$) is predicted. Of considerable current interest is the generality with which any theoretical approach is capable of predicting the salt-insensitivity of S_aK_{obs} that has been reported in experimental studies of the binding of oligocations to polymeric nucleic acids. Extensive thermodynamic data recently have become available for the binding of oligolysines L^{z+} ($3 \le Z \le 10$) to single-stranded polynucleotides (Mascotti and Lohman, 1990, 1992). As yet only limited experimental data are available for binding of an octalysine to a polymeric double-helical nucleic acid (Latt and Sober, 1967; cf. Record et al., 1976), although additional experimental determinations of K_{obs} for binding of octalysine to long and short B-DNA oligomers are in progress in this laboratory (Zhang et al., manuscript in preparation). GCMC predictions of S_aK_{obs} for binding of L^{8+} to polymeric B-DNA over a wide range of $a_\pm$ will be reported in a subsequent paper (Bond et al., manuscript in preparation). GCMC simulations for other ligand valences and for single-stranded nucleic acid N-mers are in progress.

We thank Pam Mills for helpful discussions, and Sheila Aiello for her assistance in preparing the manuscript.

This study was made possible by a generous grant of supercomputer time from SDSC (La Jolla) and the support of National Institutes of Health grant GM34351.

REFERENCES

Allen, M. P., and D. J. Tildesley. 1987. Computer Simulation of Liquids. Oxford University Press, New York.

Anderson C. F., and M. T. Record, Jr. 1980. The relationship between the Poisson-Boltzmann model and the condensation hypothesis: an analysis based on the low salt form of the Donnan coefficient. *Biophys. Chem.* 11:353–360.

Anderson C. F., and M. T. Record, Jr. 1982. Polyelectrolyte theories and their applications to DNA. *Annu. Rev. Phys. Chem.* 33:191–222.

Anderson C. F., and M. T. Record, Jr. 1983. The thermodynamic effects of polyelectrolyte-electrolyte interactions. *In* Structure and Dynamics: Nucleic Acids and Proteins. E. Clementi and R. Sarma, editors. Adenine Press, New York. 301–319.

Anderson C. F., and M. T. Record, Jr. 1990. Ion distributions around DNA and cylindrical polyions: theoretical descriptions and physical implications. *Annu. Rev. Biophys. Biophys.* 19:423–465.

Anderson, C. F., and M. T. Record, Jr. 1993. The salt-dependence of oligoion-polyion binding: a thermodynamic description based on preferential interaction coefficients. *J. Phys. Chem.* 97:7116–7126.

Anderson, S. L. 1990. Random number generators on vector supercomputers and other advanced architectures. *SIAM Rev.* 32:221–251.

Bacquet, R. J., and P. J. Rossky. 1984. Ionic atmosphere of rodlike polyelectrolytes: a hypernetted chain study. *J. Phys. Chem.* 88: 2660–2669.

Bond, J. P., C. F. Anderson, and M. T. Record, Jr. 1994. Conformational transitions of duplex and triplex nucleic acid helices: thermodynamic analysis of effects of salt concentration on stability using preferential interaction coefficients. *Biophys. J.* 67:825–836.

Braunlin, W. H. 1995. NMR Studies of Cation Binding Environments on Nucleic Acids. In press.

Elson, E. L., I. E. Scheffler, and R. L. Baldwin. 1970. Helix formation by d(TA) oligomers. III. Electrostatic effects. *J. Mol. Biol.* 54:401–415.

Fixman, M. 1979. The Poisson-Boltzmann equation and its application to polyelectrolytes. *J. Chem. Phys.* 70:4995–5005.

Fritsch, V. G. Ravishanker, D. L. Beveridge, and E. Westhof. 1993. Molecular dynamics simulations of poly(dA)·poly(dT): comparisons between implicit and explicit solvent representations. *Biopolymers.* 33:1537–1552.

Hastings, W. K. 1970. Monte Carlo sampling methods using Markov chains and their applications. *Biometrika.* 57:97–109.

Jayaram, B., and D. L. Beveridge. 1991. Grand canonical Monte Carlo simulations of aqueous solutions of NaCl and NaDNA: excess chemical potentials and sources of nonideality in electrolyte and polyelectrolyte solutions. *J. Phys. Chem.* 95:2506–2516.

Jayaram, B., S. Swaminathan, D. L. Beveridge, K. Sharp, and B. Honig. 1990. Monte Carlo simulation studies on the structure of the counterion atmosphere of B-DNA. Variations on the primitive dielectric model. *Macromolecules.* 23:3145–3165.

Katoh, T., and T. Ohtsuki. 1982. End effects for a rodlike polyelectrolyte molecule in salt solution. *J. Polymer Sci.* 20:2167–2175.

Klein, B. J., and G. R. Pack. 1983. Calculations of the spatial distribution of charge density in the environment of DNA. *Biopolymers.* 22:2331–2352.

Latt, S. A., and H. A. Sober. 1967. Protein-nucleic acid interactions. II. Oligopeptide-polyribonucleotide binding studies. *Biochemistry.* 6:3293–3306.

Laughton, C. A., and S. Neidle. 1992. Molecular dynamics simulation of the DNA triplex $d(TC)_5 \cdot d(GA)_5 \cdot d(C^+T)_5$. *J. Mol. Biol.* 223:519–529.

Lohman, T. M., and D. P. Mascotti. 1992. Thermodynamics of ligand-nucleic acid interactions. *Methods Enzymol.* 212:400–424.

Manning, G. 1969. Limiting laws and counterion condensation in polyelectrolyte solutions. *J. Chem. Phys.* 51:924–933.

Mascotti, D. P., and T. M. Lohman. 1990. Thermodynamic extent of counterion release upon binding oligolysines to single-stranded nucleic acids. *Proc. Natl. Acad. Sci. USA.* 87:3142–3146.

Mascotti, D. P., and T. M. Lohman. 1992. Thermodynamics of single-stranded RNA binding to oligolysines containing tryptophan. *Biochemistry.* 31:8932–8946.

Mills, P., C. F. Anderson, and M. T. Record, Jr. 1985. Monte Carlo studies of counterion-DNA interactions. Comparison of the radial distribution of counterions with predictions of other polyelectrolyte theories. *J. Phys. Chem.* 89:3984–3994.

Mills, P., C. F. Anderson, and M. T. Record, Jr. 1986. Grand canonical Monte Carlo calculations of thermodynamic coefficients for a primitive model of DNA-salt solutions. *J. Phys. Chem.* 90:6541–6548.

Misra, V. K., K. A. Sharp, R. A. Friedman, and B. Honig. 1994. Salt effects on ligand-DNA binding. Minor groove binding antibiotics. *J. Mol. Biol.* 238:245–263.

Mohan, V., P. E. Smith, and B. M. Pettitt. 1993. Molecular dynamics simulation of ions and water around triplex DNA. *J. Phys. Chem.* 97:12984–12990.

Murthy, C. S., R. J. Bacquet, and P. J. Rossky. 1985. Ionic distributions near polyelectrolytes: a comparison of theoretical approaches. *J. Phys. Chem.* 89:701–710.

Olmsted, M. C. 1991. Grand canonical Monte Carlo analysis of the thermodynamics of processes involving oligomeric and polymeric DNA. Ph. D. Thesis, University of Wisconsin-Madison.

Olmsted, M. C., C. F. Anderson, and M. T. Record, Jr. 1989. Monte Carlo description of oligoelectrolyte properties of DNA oligomers: range of the end effect and the approach of molecular and thermodynamic properties to the polyelectrolyte limits. *Proc. Natl. Acad. Sci. USA.* 86:7766–7770.

Olmsted, M. C., C. F. Anderson, and M. T. Record, Jr. 1991. Importance of oligoelectrolyte end effects for the thermodynamics of conformational transitions of nucleic acid oligomers: a grand canonical Monte Carlo analysis. *Biopolymers.* 31:1593–1604.

Olmsted, M. C., and P. Hagerman. 1995. Excess counterion accumulation around branched nucleic acids. *J. Mol. Biol.* In press.

Padmanabhan, S., V. M. Brushaber, C. F. Anderson, and M. T. Record, Jr. 1991. Relative affinities of divalent polyamines and of their N-methylated analogs for helical DNA determined by ^{23}Na NMR. *Biochemistry.* 30: 7550–7559.

Padmanabhan, S., M. Paulsen, C. F. Anderson, and M. T. Record, Jr. 1990. Cation-DNA interactions: NMR and theoretical studies of ion distributions and dynamics. *In* Monovalent Cations in Biological Systems, Chapter 14. C. Pasternak, editor. CRC Press, Boca Raton, FL. 321–338.

Record, M. T., Jr., and C. F. Anderson. 1995. Interpretation of preferential interaction coefficients of nonelectrolytes, and of electrolyte ions in terms of a two domain model. *Biophys. J.* In press.

Record, M. T. Jr., C. F. Anderson, and T. M. Lohman. 1978. Thermodynamic analysis of ion effects on the binding and conformational equilibria of proteins and nucleic acids: the roles of ion association or release, screening, and ion effects on water activity. *Q. Rev. Biophys.* 11:102–178.

Record, M. T. Jr., J.-H. Ha, and M. Fisher. 1991. Use of equilibrium and kinetic measurements to determine the thermodynamic origins of stability and specificity and mechanism of formation of site specific complexes between proteins and helical DNA. *Methods Enzymol.* 208:291–343.

Record, M. T. Jr., and T. M. Lohman. 1978. A semiempirical extension of polyelectrolyte theory to the treatment of oligoelectrolytes: application to oligonucleotide helix-coil transitions. *Biopolymers.* 17:159–166.

Record, M. T. Jr., T. M. Lohman, and P. L. DeHaseth. 1976. Ion effects on ligand-nucleic acid interactions. *J. Mol. Biol.* 107:145–158.

Record, M. T. Jr., M. Olmsted, and C. F. Anderson. 1990. Theoretical studies of the thermodynamic consequences of interactions of ions with polymeric and oligomeric DNA. *In* Theoretical Biochemistry and Molecular Biophysics. D. L. Beveridge and R. Lavery, editors. Adenine Press, New York. 285–307.

Record, M. T. Jr., and B. Richey. 1988. Physical chemical analysis of biopolymer self-assembly interactions. *In* ACS Sourcebook for Physical Chemistry Instructors. T. Lippincott, editor. American Chemical Society. Washington, D.C. 145–159.

Schildkraut C., and S. Lifson. 1965. Dependence of the melting temperature of DNA on salt concentration. *Biopolymers.* 3:195–208.

Seibel, G. L., U. C. Singh, and P. A. Kollman. 1985. A molecular dynamics simulation of double-helical B-DNA including counterions and water. *Proc. Natl. Acad. Sci. USA.* 82:6537–6540.

Stein, V. M., J. P. Bond, M. W. Capp, C. F. Anderson, and M. T. Record, Jr. 1995. Importance of coulombic end effects on cation accumulation near oligoelectrolyte B-DNA: a demonstration using ^{23}Na NMR. *Biophys. J.* In press.

Stigter, D. 1975. The charged colloidal cylinder with a Gouy double layer. *J. Colloid Interface Sci.* 53:296–306.

Swaminathan, S., G. Ravishanker, and D. L. Beveridge. 1991. Molecular dynamics of B-DNA including water and counterions: a 140-ps trajectory for d(CGCGAATTCGCG) based on the GROMOS force field. *J. Am. Chem. Soc.* 113:5017–5040.

Valleau, J. P., and K. L. Cohen. 1980. Primitive model electrolytes I. Grand canonical Monte Carlo computations. *J. Chem. Phys.* 72:5935–5941.

Valleau, J. P., and S. G. Whittington. 1977. Guide to Monte Carlo for statistical mechanics: 1. Highways. *In* Modern Theoretical Chemistry, Vol. 5A. B. J. Berne, editor. Plenum Press, New York. 137–168.

van Gunsteren, W. F., H. J. C. Berendsen, R. G. Geurtsen, and H. R. J. Zwinderman. 1986. A molecular dynamics computer simulation of an eight-base-pair DNA fragment in aqueous solution: comparison with experimental two-dimensional NMR data. *Ann. N. Y. Acad. Sci.* 482:287–303.